*Catalysis Letters Vol. 105, Nos. 3–4, December 2005 (© 2005)*
DOI: 10.1007/s10562-005-8685-6


# $Cu–ZrO_2$ catalysts for water-gas-shift reaction at low temperatures

Jung Bong Ko, Chul Min Bae, You Shick Jung, and Dong Hyun Kim*

*Department of Chemical Engineering, Kyungpook National University, Daegu, 702-701 Korea*

Received 19 August 2005; accepted 19 August 2005

A series of $Cu–ZrO_2$ catalysts with Cu content in the range of 10–70 at.% Cu (=100×Cu/(Cu + Zr)) were prepared by coprecipitation, and their performances were tested for the water-gas-shift (WGS) reaction. The activity of the catalyst increased with Cu loading and, depending on the loading, the activity was comparable to or better than the activity of a conventional $Cu–ZnO–Al_2O_3$ catalyst at low temperatures below 473 K. Characterization of the catalysts revealed that the amount of $Cu^+$ present on the catalyst surface, after being reduced by a $H_2$ mixture at 573 K, was well correlated with the activity of the catalyst, indicating that the $Cu^+$ species were the active sites of the WGS reaction. The easy redox between $Cu^{2+}$ and $Cu^+$ during the WGS reaction was considered to be responsible for the high activity of $Cu–ZrO_2$ at low temperatures. A reaction mechanism based on the redox was proposed.

**KEY WORDS:** water-gas-shift reaction; $Cu–ZrO_2$ catalyst; active site; reaction mechanism.

## 1. Introduction

$Cu–ZrO_2$ catalysts have received increasing attention for their promising catalytic activity in a number of reactions: methanol synthesis from mixtures of hydrogen and carbon oxides [1–3], NO reduction with hydrocarbons [4] or CO [5,6], and CO oxidation [7].

The activity of $Cu–ZrO_2$ has been discussed to originate from an interaction between copper and zirconia. The interaction resulted in a better Cu dispersion and surface area than CuO or $ZrO_2$ alone [8]. A density functional calculation revealed the electron transfer from copper to zirconia and a weakened surface hydroxyl on zirconia surface [9]. The redox state of Cu ions in $Cu–ZrO_2$ has been shown to easily undergo changes in mild conditions such as room temperature hydration [10]. The incorporation of Cu ions in the lattice position of Zr ions was reported to be responsible for the catalytic activity in $CH_4$ and CO oxidation [11]. A facilitated reduction of the Cu species was observed in temperature-programmed reduction with hydrogen or CO, and it was ascribed to a close interaction with $ZrO_2$ [12,13]. In methanol synthesis and decomposition, Cu and zirconia behaved in a bifunctional manner, with Cu serving as a site for the dissociation or removal of hydrogen molecules, and zirconia as an adsorption site for CO, $CO_2$ and all other carbon containing intermediates [2,14].

In this study, we examined the catalytic behavior of $Cu–ZrO_2$ in the water-gas-shift (WGS) reaction. Incidentally, the behavior $Cu–ZrO_2$ in WGS reaction has not been reported in the open literature, to the best of our knowledge. We observed some interesting and promising activity of the catalyst in the water-gas-shift reaction, particularly at temperatures below 473 K. Based on the experimental findings, we proposed the active site and a reaction mechanism for the WGS reaction over $Cu–ZrO_2$.

* To whom correspondence should be addressed.
E-mail: dhkim@mail.knu.ac.kr

## 2. Experimental

A series of $Cu–ZrO_2$ catalysts were prepared by the method of coprecipitation. The precursor salts $Cu(NO_3)_2{\cdot}3H_2O$ and $ZrO(NO_3)_2{\cdot}6H_2O$, were dissolved in deionized water and heated to 323 K. An NaOH solution was used to precipitate the metal components. The resulting precipitate was filtered, washed with 2000 mL of hot deionized water to remove the residual sodium and dried at 363 K for 12 h in an oven. The dried sample was calcined at 773 K for 3 h (heating rate was 5 K/min). The catalysts with 10, 20, 30, 40, 50 and 70 at.% Cu (=Cu/(Cu + Zr)×100%) were prepared. For comparison, a $Cu–ZnO–Al_2O_3$ catalyst (60 at.% Cu, 30 at.% Zn and 10 at.% Al) was prepared by the same procedures.

To estimate bulk composition, the catalysts were dissolved in a HF solution, diluted with deionized water, and analyzed by an Inductively Coupled Plasma (ICP) Atomic Emission Spectrometer (Jobin-Yvon). The surface composition was estimated by XPS (VG scientific) using a 300 W Mg $K_\alpha$ X-ray source. An XRD analysis of the catalyst sample was performed on a Phillips X-pert Diffractometer with Cu $K_\alpha$ radiation and a monochromatic detector.

TPR measurements were carried out in a conventional reactor with a programmable temperature controller and a TCD detector. The catalyst sample (100 mg) was pretreated with 10% $O_2/N_2$(50 mL/min)

at 573 K for 1 h and cooled to room temperature under $N_2$ flow. The reduction gas was a 10% $H_2/N_2$ mixture flowing at 50 mL/min and the temperature rate was 10 K/min. The TPR peak area was calibrated with the TPR peak obtained with 50 mg of CuO.

The Cu metal area was measured by the method of $N_2O$ dissociation on the catalyst samples [15]. A 150 mg sample was first reduced at 573 K for 3 h under a 10% $H_2/N_2$ mixture flowing at 50 mL/min. Then, the sample was cooled to 363 K under a He flow, and 250 $\mu$L of $N_2O$ pulses were injected in a series of 3-min intervals using He as a carrier gas (30 mL/min). The $N_2$ and $N_2O$ in the effluent were separated in a Porapak N column (1 m, 1/8 inch) at room temperature and analyzed with a TCD detector.

The CO pulse chemisorption experiment was performed at room temperature in order to measure the $Cu^+$ area of the catalyst. Prior to chemisorption, a 150 mg catalyst sample was reduced at 573 K under a 10% $H_2$/He mixture flowing at 50 mL/min. CO pulses (250 $\mu$L), carried by a He flow, were injected in a series of 3-min intervals into the reactor packed with the catalyst sample.

The reaction experiments were carried out in a stainless steel tube reactor (0.25 inch OD, 50 cm length) at atmospheric pressure and in the temperature range of 353 K $\sim$ 473 K. The catalyst (0.15–0.18 mm particles) loading was 300 mg. The reaction temperature was monitored with a K-type thermocouple placed in the middle of the catalyst bed. Before the reaction, the catalyst was reduced under a 10% $H_2/N_2$ flow (50 mL/min) at 573 K for 2 h. The feed gas was 2% CO, 10% $H_2O$ and balance $N_2$, flowing at 100 mL/min. The CO gas (99.95%) was passed through a hot quartz tube at 673 K in order to decompose the likely impurity of iron carbonyl [16]. An oxygen trap was used to remove traces of oxygen in the $N_2$ gas. The mixture of CO and $N_2$ gas (88 mL/min) was bubbled trough a saturator filled with deionized water to add water vapor into the feed stream. The saturator temperature was controlled at 318.2 K. The reactor effluent was cooled to 274 K to remove water and it was analyzed on-line by a gas chromatography (Hewlett Packard 5890A) with a TCD. A Carboxen column (Supelco I-2390) was used to separate CO and $CO_2$.

## 3. Results and discussion

Figure 1 shows the CO conversion of the catalysts with temperature for a feed of 2% CO and 10% $H_2O$. The reaction, under the experimental conditions, was virtually irreversible since the equilibrium CO conversion for the feed at 473 K is 99.96%. The CO conversion increased with the Cu content of the catalyst from 10 to 70 at.%, indicating that Cu was an active component in the catalysts. For comparison, the activity of a conventional low-temperature-shift catalyst, Cu–ZnO–$Al_2O_3$, is also shown.

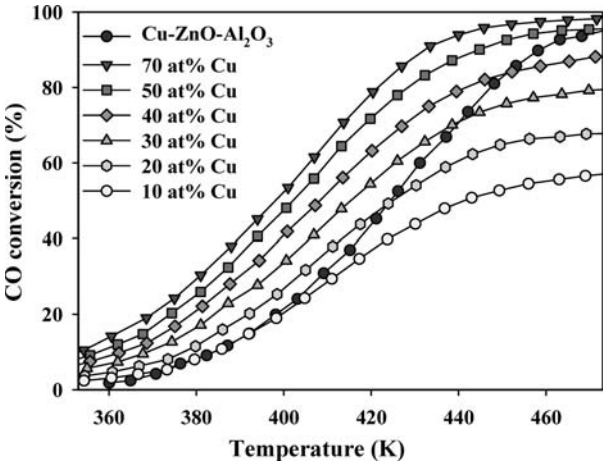


Figure 1. WGS activity of CuO–$ZrO_2$ catalysts and a Cu–ZnO–$Al_2O_3$ catalyst. Feed: 100 mL/min (2% CO, 10% $H_2O$, balance $N_2$); catalyst: 300 mg, 0.15–0.18 mm.

At temperatures lower than 380 K, all catalysts performed better than the conventional catalyst, but as the temperature increased above 380 K, the catalysts with low Cu content began to lag behind the Cu–ZnO–$Al_2O_3$ catalyst in the CO conversion. The 70 at.% Cu catalyst, however, outperformed the Cu–ZnO–$Al_2O_3$ catalyst in the whole temperature range investigated.

The XRD patterns of the catalysts are shown in figure 2. For the 10 and 20 at.% Cu catalysts, the XRD pattern did not show a CuO phase, and the major phase was cubic zirconia. This indicates that the Cu species were present in a solid solution with $ZrO_2$ or in a highly dispersed state [8]. The $ZrO_2$ peaks disappeared when the Cu content exceeded 30 at.%, showing that for the high Cu loadings, $ZrO_2$ was also finely dispersed. It was

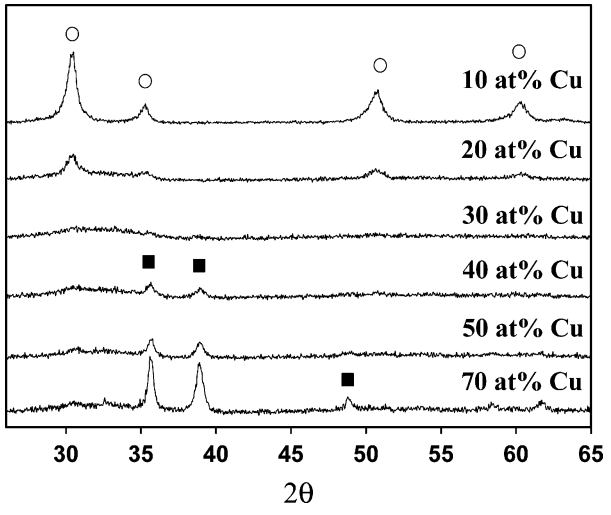


Figure 2. XRD patterns of Cu–$ZrO_2$ catalysts. (○: cubic $ZrO_2$, ■: monoclinic CuO)

reported that Cu stabilizes zirconia, both the cubic and tetragonal phases in all Cu–$ZrO_2$ compositions, and the zirconia crystallite size decreases with the Cu loading [17]. At high Cu loadings (above 40 at.%), a monoclinic CuO phase was observed.

The catalyst surface was studied by XPS. The binding energies were in the range of 933.15–933.8 eV and the shake-up peaks were present. The presence of the shake-up peaks, characteristics of the CuO species, and the range of the binding energy values, when compared with an XPS database [18], indicated that the surface Cu species were present as CuO, in agreement with previous XPS results [3,11].

The surface composition from the XPS analysis and the bulk composition analyzed by ICP are listed in table 1. It is seen that for the 10, 20 and 70 at.% Cu catalysts, the surface composition did not differ significantly from the bulk composition, while for the 30, 40 and 50 at.% catalysts, the Cu content on the surface was 5–9% lower than the bulk composition, indicating a slight enrichment of $ZrO_2$ on the surface in the intermediate Cu loadings.

The TPR profiles of the catalysts are shown in figure 3. In comparison with the TPR of CuO, the reduction of the catalysts occurred at much lower temperatures owing to the interactions between Cu oxides and $ZrO_2$. The temperature of the peak maximum increased considerably with Cu loading, from 438 K for the 10 at.% Cu–$ZrO_2$ to 518 K for the 70 at.% Cu–$ZrO_2$, indicating that the state of Cu changed with the Cu loading. Apparently, two peaks are compounded in the TPR with the Cu loading of 40 and 30 at.%. Liu et al. [3] also discerned two peaks in their TPR of the Cu–$ZrO_2$ catalysts and assigned the lower temperature peak to the CuO which strongly interacts with $ZrO_2$ and the higher temperature peak to the CuO which has little interaction with $ZrO_2$. In this regard, the increase of the peak temperature with Cu loading indicates diminishing interactions between the Cu oxides and $ZrO_2$. When compared to the profile of Cu–ZnO–$Al_2O_3$, 70 at.% Cu–$ZrO_2$ showed a similar peak height, shape and a peak maximum temperature. Nevertheless, the two catalysts exhibited considerably different CO conversion profiles, which are shown in figure 1. This suggests that although the reducible Cu species of the two catalysts were similar from the standpoint of the TPR, the catalytic role of the Cu species in WGS were different due to different electronic and geometric interactions of the Cu species with ZnO or $ZrO_2$.

The reduction peak area was calibrated with the TPR of a known amount of CuO. The extent of the reduction for each catalyst, based on the assumption that all Cu species in the catalysts were present as CuO and the reduction produced metallic Cu, is listed in table 1. The extent of reduction increased with the Cu loading, from 53.2% for the 10 at.% Cu catalyst to 75.7% for the 70 at.% Cu catalyst. This shows that although $ZrO_2$ in the catalysts facilitated reduction of a part of the Cu species, it also stabilized the remaining part of the Cu in the catalysts. It was reported that some amount of Cu can be incorporated into the zirconia lattice, and these isolated $Cu^{2+}$ ions, substituted in the framework sites of $Zr^{4+}$, are difficult to reduce, even at 973 K with hydrogen [17]. In this regard, the extent of reduction can be interpreted as the fraction of copper outside the framework of the zirconia lattice.

The Cu metal area of the catalyst was measured by the method of $N_2O$ dissociation and shown in figure 4. The measured metal area increased with Cu loading up to 10 at.%, but decreased with a further increase in the Cu loading from 10 to 70 at.%. This was unexpected in view of the XPS data which showed an increase in the surface Cu content with the Cu loading. Breen and Ross [19] reported on the Cu metal areas measured by $N_2O$ dissociation for their Cu–$ZrO_2$ catalysts: 3.0 and 3.7 $m^2/g$ for 30 at.% Cu and 70 at.% Cu catalyst, respectively, thus showing a small change in the measured metal area despite of a significant increase in the Cu loading. Morterra et al. [10] have experimentally shown that the re-oxidation of the $Cu^0$ sites on Cu–$ZrO_2$ requires the action of $O_2$ at high temperatures. This indicates that $N_2O$ titration at 363 K could not oxidize all surface $Cu^0$ sites on the Cu–$ZrO_2$ catalysts and thus was unable to provide the Cu metal area of the Cu–$ZrO_2$ catalysts. It is, however, difficult to understand the decrease in the amount of $N_2O$ titration with the Cu loading above 10 at.%.

Table 1
Catalyst characterization

| Catalyst (at.% Cu) | BET surface area ($m^2/g$) | Surface composition[a] (at.% Cu) | Bulk composition[b] (at.% Cu) | Extent of reduction[c] (%) |
|---|---|---|---|---|
| 10 | 85 | 13 | 12 | 53 |
| 20 | 112 | 23 | 22 | 54 |
| 30Cu | 114 | 27 | 32 | 66 |
| 40 | 109 | 33 | 42 | 64 |
| 50 | 105 | 47 | 52 | 74 |
| 70 | 116 | 67 | 69 | 75 |

[a]measured by XPS.
[b]measured by ICP.
[c]calculated from TPR peak area.

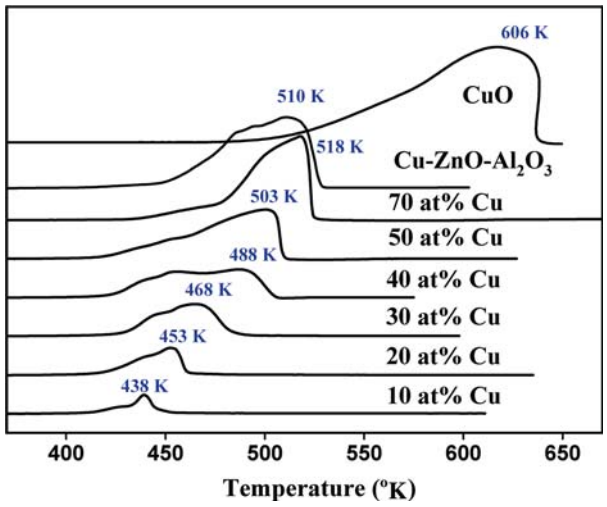


Figure 3. $H_2$-TPR of Cu–$ZrO_2$ catalysts. Condition: 50 mL/min, 5% $H_2$/He, 10 K/min; catalyst: oxidized at 573 K for 1 h with $O_2$, 0.15–0.18 mm, 100 mg.

At room temperatures, CO is easily desorbed from the $Cu^0$ and $Cu^{+2}$ sites, but it is strongly adsorbed on the $Cu^{+1}$ sites with a stoichiometry of $CO:Cu^{+1} = 1:1$ [20]. The adsorption of CO on $ZrO_2$ is reported to be reversible at room temperature [21]. Hence, CO chemisorption can be used to measure the amount of surface $Cu^{+1}$ sites on the catalysts. Figure 4 shows the amount of CO chemisorbed on the catalysts after reduction at 573 K for 3 h. The amount of $Cu^{+1}$ increased with Cu loading in the catalyst, similar to the increase in the catalytic activity with the Cu content, indicating that the amount of $Cu^{+1}$ could be related to the catalytic activity. To examine this, the turnover frequency (TOF) based on the number of the surface $Cu^{+1}$ site was calculated from the reaction rate measured by operating the reactor in a differential mode and is listed in table 2. For all catalysts, the TOF at 353 K was in the range of 0.012–0.015 $s^{-1}$ and at 373 K, it was in the range of 0.026–0.034 $s^{-1}$. These TOF numbers may indicate that $Cu^+$ is the active site of the WGS reaction.

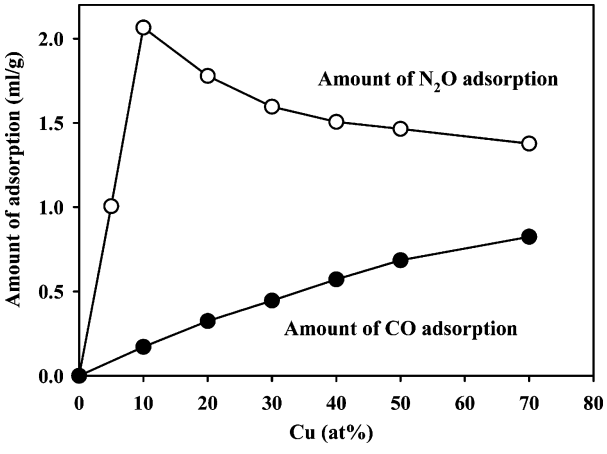


Figure 4. Effect of bulk copper content in Cu–$ZrO_2$ catalyst on the amount of $N_2O$ dissociation and CO pulse chemisorption. Catalyst: 0.15–0.18 mm, 150 mg; pretreatment: reduction at 573 K for 3 h.

Table 2
Turnover frequency of CuO–$ZrO_2$ catalysts

| Catalyst | TOF at 353 K ($s^{-1}$) | TOF at 373 K ($s^{-1}$) |
|---|---|---|
| 10 at.% Cu | 0.015 | 0.034 |
| 20 at.% Cu | 0.012 | 0.027 |
| 30 at.% Cu | 0.013 | 0.026 |
| 40 at.% Cu | 0.012 | 0.029 |
| 50 at.% Cu | 0.013 | 0.032 |
| 70 at.% Cu | 0.013 | 0.031 |

Feed: 100 mL/min (2% CO, 10% $H_2O$ and balance $N_2$).

The redox state of Cu ions in Cu–$ZrO_2$ easily underwent changes in mild reductive or oxidative conditions, and the hydration of the catalyst even at room temperature efficiently oxidized $Cu^+$ to $Cu^{2+}$ [10]. The highly dispersed $Cu^{2+}$ species in Cu–$ZrO_2$ were reduced to $Cu^+$ by CO at a low temperature around 373 K [22]. On the basis of the TOF data and the literature results, the reaction mechanism of Cu–$ZrO_2$, during the WGS reaction below 473 K, is proposed in figure 5. In the mechanism, CO reduces $Cu^{2+}$ to $Cu^+$ and produces $CO_2$, while $H_2O$ oxidizes $Cu^+$ to $Cu^{2+}$ and generates $H_2$. It is considered that the facilitated change in the oxidation states between $Cu^{2+}$ and $Cu^+$ over the Cu–$ZrO_2$ catalyst is responsible for the excellent low-temperature activity of the Cu–$ZrO_2$ catalysts in the WGS reaction.

## 4. Conclusion

A series of Cu–$ZrO_2$ catalysts were prepared by co-precipitation and tested for the water-gas-shift reaction at low temperatures. Compared to a Cu–ZnO–$Al_2O_3$ catalyst, the Cu–$ZrO_2$ catalysts showed an excellent performance in the reaction, and the activity of the catalyst increased with the Cu loading. At low Cu loadings below 40 at.%, Cu was present in the form of highly dispersed oxide clusters, while at high loadings, the clusters as well as bulk CuO were present in the catalysts. In $H_2$-TPR, $ZrO_2$ was seen to increase the reducibility of a part of the Cu oxides, but it was also seen to stabilize the Cu oxides in close contact with $ZrO_2$. A stable $Cu^{+1}$ species was shown to be present on the catalyst surface even after reducing the catalyst at 573 K under a hydrogen mixture, and its amount,

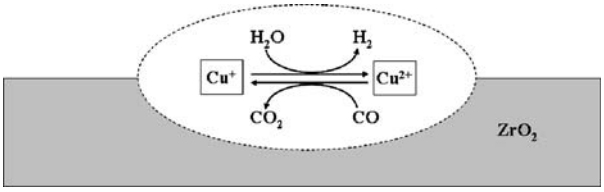


Figure 5. Proposed reaction mechanism for water-gas-shift reaction over Cu–$ZrO_2$.

measured by CO pulse chemisorption, was in good correlation with the activity of the Cu–$ZrO_2$ catalyst, indicating the stable $Cu^+$ after the reduction is the active site for the reaction. A reaction mechanism based on the redox between $Cu^{2+}$ and $Cu^+$ is proposed for the water-gas-shift reaction with the Cu–$ZrO_2$ catalysts.

## Acknowledgment

This work was supported by the Hydrogen Energy R&D Center at Korea Institute of Energy and Resources, Daejun, Korea.

## References

[1] R.A. Koeppel, A. Baiker and A. Wokaun, Appl. Catal. A 84 (1992) 77.
[2] I.A. Fisher, H.C. Woo and A.T. Bell, Catal. Lett. 44 (1997) 11.
[3] J. Liu, J. Shi, D. He, Q. Zhang, X. Wu, Y. Liang and Q. Zhu, Appl. Catal. A 218 (2001) 113.
[4] H. Aritani, S. Kawaguchi, T. Yamamoto, T. Tanaka, Y. Okamoto and S. Imamura, Chem. Lett. 29 (2000) 532.
[5] N. Mizuno, M. Yamato, M. Tanaka and M. Misono, J. Catal. 132 (1991) 560.
[6] Y. Okamoto, T. Kubota, H. Gotoh, Y. Ohto, H. Aritani, T. Tanaka and S. Yoshida, J. Chem. Soc. Faraday Trans. 94 (1998) 3743.
[7] W.P. Dow and T.J. Huang, J. Catal. 147 (1994) 322.
[8] S. Kikuyama, A. Miura, R. Kikuchi, T. Takeguchi and K. Eguchi, Appl. Catal. A 259 (2004) 191.
[9] G. Wu, Y. Sun, Y.W. Li, H. Jiao, H.W. Xiang and Y. Xu, J. Mol. Struct. 626 (2003) 287.
[10] C. Morterra, E. Giamello, G. Cerrato, G. Centi and S. Perathoner, J. Catal. 179 (1998) 111.
[11] M.K. Dongare, V. Ramaswamy, C.S. Gopinath, A.V. Ramaswamy, S. Scheurell, M. Brueckner and E. Kemnitz, J. Catal. 199 (2001) 209.
[12] L. Kundakovic and M. Flytzani-Stephanopoulos, Appl. Catal. A 171 (1998) 13.
[13] R. Zhou, T. Yu, X. Jiang, F. Chen and X. Zheng, Appl. Surf. Sci. 148 (1999) 263.
[14] I.A. Fisher and A.T. Bell, J. Catal. 184 (1999) 357.
[15] J.W. Evans, M.S. Wainwright, A.J. Bridgewater and D.J. Young, Appl. Catal. 7 (1983) 75.
[16] D.D. Perrin, W.L.F. Armarego and D.R. Perrin, *Purification of Laboratory Chemical* (Pergamon Press, Oxford, 1996).
[17] V. Ramaswamy, M. Bhagwat, D. Srinivas and A.V. Ramaswamy, Catal. Today 97 (2004) 63.
[18] NIST (National Institute of Science and Technology) X-ray Photoelectron Spectroscopy Database. http://srdata.nist. gov/xps/.
[19] J.P. Breen and J.R.H. Ross, Catal. Today 51 (1999) 521.
[20] A. Dandekar and M.A. Vannice, J. catal. 178 (1998) 621.
[21] X. Mugniery, T. Chafik, M. Primet and D. Bianchi, Catal. Today 52 (1999) 15.
[22] Y. Okamoto, H. Gotoh, H. Aritani, T. Tanaka and S. Yoshida, J. Chem. Soc. Faraday trans. 93 (1997) 3879.